INORGANIC CHEMISTRY
FRONTIERS

RESEARCH ARTICLE

View Article Online
View Journal | View Issue

Cite this: *Inorg. Chem. Front.*, 2024, **11**, 3254

Phase switching and shape-memory effect in a molecular material: revisiting the Werner complex $[Ni(4\text{-}MePy)_4(NCS)_2]$†

Shi-Qiang Wang, *[a] Shaza Darwish, [b] Catiúcia R. M. O. Matos, [b] Zicong Marvin Wong, [c] Anjaiah Nalaparaju, [c] Yifei Luo, [a] Jun Zhu, [a] Xiaofei Zhang, [a] Zhengtao Xu*[a] and Michael J. Zaworotko *[b]

Received 11th March 2024,
Accepted 18th April 2024

DOI: 10.1039/d4qi00636d

rsc.li/frontiers-inorganic

Shape-memory effects and stimuli-induced phase transformations are observed across many types of materials but remain understudied in molecular materials. In this contribution, we revisit the Werner complex, $[Ni(4\text{-}MePy)_4(NCS)_2]$ (4-MePy = 4-methylpyridine), a molecular material that has long been known to form Werner clathrates and possess a porous polymorph. Whereas earlier work implied that $[Ni(4\text{-}MePy)_4(NCS)_2]$ could be a shape-memory material, we confirmed this to be the case through *p*-xylene (PX) vapor sorption studies. Specifically, $[Ni(4\text{-}MePy)_4(NCS)_2]$ transformed from its reported nonporous **α** phase to the PX-loaded **β** phase induced by PX vapour. **β** reversibly transformed to its porous **β′** phase upon PX removal over at least three PX sorption cycles. **β′** reverted to **α** upon heating at 80 °C in a closed vessel. The porosity of **β′** was explored by examining its C_3H_x (x = 4, 6, and 8) gas sorption properties, which revealed guest size/shape-dependent sorption behaviour with uptakes of 0.6, 0.9 and 1.6 mol mol^{-1} for C_3H_8, C_3H_6 and C_3H_4, respectively. Insight into the structural transformations of the **α**, **β**, and **β′** phases is provided by analysis of their previously reported crystal structures and new density functional theory calculations.

Introduction

Soft porous crystals that exhibit guest-induced structural transformations,[1,2] especially flexible metal–organic materials (FMOMs),[3–11] are of interest thanks to their potential utility in gas storage[12–16] and hydrocarbon separation.[17–22] A feature of some FMOMs is that they can undergo reversible structural transformation(s) between their activated (desolvated) and guest-loaded phases induced by guest sorption,[23–30] often with varying levels of hysteresis.[12–22,31–36]

The shape-memory effect (SME) is a related phenomenon whereby a shape-memory material (SMM) transforms to a new polymorphic morphology in response to an external stimulus (typically mechanical stress), reverting to its original phase only when subjected to a different external stimulus (usually heat).[37] While certain classes of SMMs, like shape-memory alloys and polymers, have found applications in various device components such as actuators, valves, connectors, seals, and self-torquing fasteners,[38–40] the exploration of SMMs in the domain of FMOMs is much less developed.

In principle, should FMOMs exhibit structural transformations between polymorphic phases, then they could also function as SMMs (Scheme 1). Indeed, recent studies have demon-

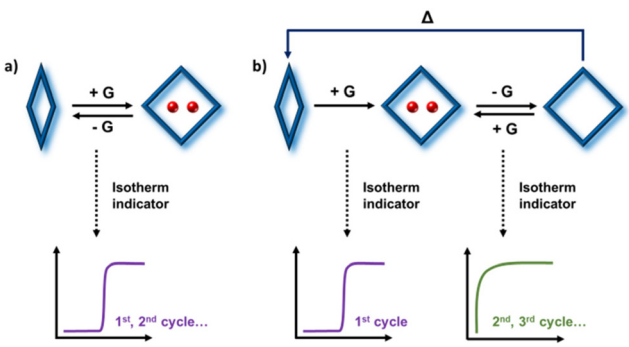

Scheme 1 Illustration of FMOMs with (a) reversible and (b) "shape-memory" type phase transformation induced by guest (G) sorption, distinguished by their successive sorption isotherm profiles.

[a]*Institute of Materials Research and Engineering (IMRE), Agency for Science, Technology and Research (A*STAR), 2 Fusionopolis Way 138634, Singapore. E-mail: wangsq@imre.a-star.edu.sg, zhengtao@imre.a-star.edu.sg*
[b]*Bernal Institute, Department of Chemical Sciences, University of Limerick, Limerick V94 T9PX, Republic of Ireland. E-mail: xtal@ul.ie*
[c]*Institute of High Performance Computing (IHPC), Agency for Science, Technology and Research (A*STAR), 1 Fusionopolis Way 138632, Singapore*

†Electronic supplementary information (ESI) available: TGA curves, PXRD patterns, SEM images, *etc*. See DOI: https://doi.org/10.1039/d4qi00636d

strated the SME in a handful of 3D FMOMs,[41–47] as evidenced by their successive sorption isotherms. Despite these encouraging findings, the SME remains an underexplored phenomenon in molecular FMOMs, with only one known example, a platinum(II)–diimine complex that was studied for its vapochromic shape-memory characteristics.[48]

In this context, we have recently explored guest-induced structural transformations of Werner complexes and termed them as *switching adsorbent molecular materials* (SAMMs).[49,50] To the best of our knowledge, the first phase switching transformation among FMOMs was observed in a SAMM, the Werner complex [Co(4-ethylpyridine)$_4$(NCS)$_2$] (SAMM-1-Co-NCS), dating back to 1969.[51] The gas/vapor sorption properties of other Werner complexes remains understudied. It was not until over 40 years later that several Werner complexes, featuring different metal ions, pyridyl ligands and axial anions, were found to exhibit similar guest-induced phase switching.[49,52–55] This motivated us to investigate the Ni analogue of SAMM-1-Co-NCS with a shorter ligand, [Ni(4-MePy)$_4$(NCS)$_2$] (4-MePy = 4-methylpyridine), with respect to its switching behaviour and shape-memory effect through a literature survey of its reported crystal structures and sorption studies with *p*-xylene (PX) vapour and C_3H_x (x = 4, 6, or 8) gases.

[Ni(4-MePy)$_4$(NCS)$_2$] is one of the earliest and most extensively studied Werner complexes.[56,57] Its nonporous **α** phase was synthesized in 1952,[58] with the crystal structure determined 25 years later in 1977.[59] [Ni(4-MePy)$_4$(NCS)$_2$]-**α** was later used for the separation of xylenes, cymenes, and other isomers thanks to its inclusion selectivity for aromatic compounds.[60,61] A number of the resulting Werner clathrates were found to crystallize in the tetragonal space group $I4_1/a$ (Table S1†) and adopt a channel-type (**β** phase) packing motif.[62–65] Interestingly, the methanol or benzene-loaded **β** phase was reported to retain permanent porosity after guest removal,[51,65] and the crystal structure of this activated **β′** phase was determined in 1972.[66] It was also noted that [M(4-MePy)$_4$(NCS)$_2$]-**α** (M = Co, Ni, *etc.*) can transform to the **β** form when exposed to aromatic hydrocarbons as confirmed by powder X-ray diffraction (PXRD),[51,67,68] although dynamic vapor sorption measurements remain to be reported. With the above information in mind, [Ni(4-MePy)$_4$(NCS)$_2$] may be considered as a likely SMM, even though it has not yet been verified as such. Given that successive sorption isotherms can be useful for identifying potential SMMs and mapping the transformation landscape (Scheme 1), we undertook a systematic study of the transformations of [Ni(4-MePy)$_4$(NCS)$_2$] through successive PX vapor sorption experiments, complemented by C3 gas sorption studies and density functional theory (DFT) calculations.

Results and discussion

[Ni(4-MePy)$_4$(NCS)$_2$]-**α** was synthesized as a microcrystalline powder (0.5–3 μm rod-like morphology, Fig. S1†) using a water slurry method described earlier.[58,60] Single crystals (SCs) were obtained by recrystallization from hot ethanol. The crystal structure comprises discrete propeller-shaped molecules, with Ni cations octahedrally coordinated to the N atoms of two axial isothiocyanate ligands and four equatorial pyridyl ligands (Fig. 1a). Calculated and experimental PXRD patterns of [Ni(4-MePy)$_4$(NCS)$_2$]-**α** are given in Fig. 1b. For the as-synthesized powder sample (magenta line) and ground SC sample (blue line), a high intensity peak at 2θ = 9.35° was observed. This peak is systematically absent in the calculated PXRD pattern (black line) and the experimental PXRD pattern of the unground SC sample (red line). Another possibility that cannot be excluded is polymorphism, a phenomenon observed in crystalline materials where two or more dense phases may exist.[69,70] Thermogravimetric analysis (TGA) indicated thermal stability of [Ni(4-MePy)$_4$(NCS)$_2$]-**α** up to 100 °C under N_2 (Fig. S2†). Additionally, water vapor sorption (Fig. S3†) revealed the hydrophobic nature of [Ni(4-MePy)$_4$(NCS)$_2$]-**α**, with the gradual but low water uptake (<1 wt%) attributed to surface sorption.

PX vapor sorption isotherms were collected at 298 K for both the as-synthesised powder and recrystallized SC forms of [Ni(4-MePy)$_4$(NCS)$_2$]-**α** and revealed clear switching behaviour (Fig. 2b), making it a new member of SAMMs. In addition, we noticed that the as-synthesised powder and recrystallized SC samples exhibited different switching pressure thresholds and sorption profiles. The as-synthesised powder sample exhibited a step at 30% P/P_0 and a smaller step at 60% P/P_0, while the recrystallized SC sample displayed a single step at 45% P/P_0 and substantially lacked such a sub-step in its sorption isotherm. These differences could be attributed to factors such as crystallinity, particle size, and polymorphic effects, which have been previously observed in several FMOMs.[41,71–75]

Both forms of [Ni(4-MePy)$_4$(NCS)$_2$]-**α** exhibited PX uptake of 18.9 wt% at 95% P/P_0, consistent with a composition of one PX molecule per host molecule as reported in the crystal structure of [Ni(4-MePy)$_4$(NCS)$_2$]-PX (Fig. 2a).[62] Notably, the phase transformation was complete within 10 minutes once the switching pressure threshold had been reached, as revealed by the sorption kinetics testing (Fig. S4†). The PX desorption branches exhibited large hysteresis, with PX not being released until 0%

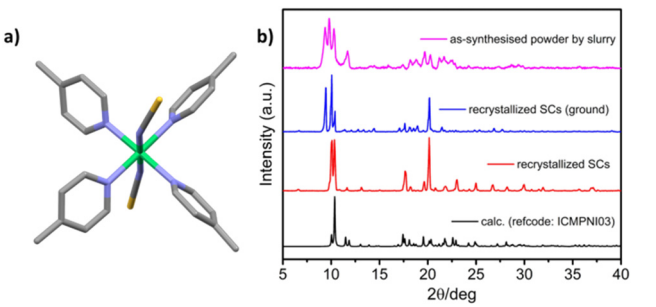

Fig. 1 (a) Crystal structure of [Ni(4-MePy)$_4$(NCS)$_2$]-**α**. Green: Ni, blue: N, grey: C, yellow: S. Hydrogen atoms are omitted for clarification (the same hereafter). (b) Calculated and experimental PXRD patterns of [Ni(4-MePy)$_4$(NCS)$_2$]-**α**. (SCs = single crystals).

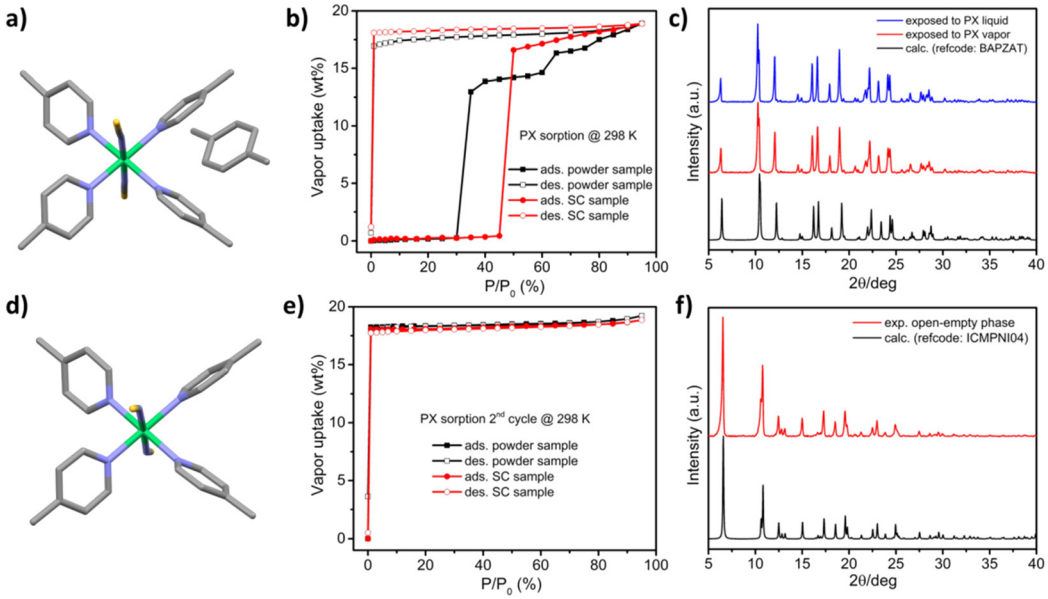

Fig. 2 (a and d) Crystal structures of [Ni(4-MePy)$_4$(NCS)$_2$]-PX and [Ni(4-MePy)$_4$(NCS)$_2$]-**β′**, respectively; (b and e) the first and second cycles of PX vapor sorption isotherms (298 K) of the as-synthesised powder and recrystallized SC samples of [Ni(4-MePy)$_4$(NCS)$_2$]-**α**; (c) experimental PXRD patterns for [Ni(4-MePy)$_4$(NCS)$_2$]-**α** exposed to PX vapor or liquid and comparison with the calculated PXRD pattern of [Ni(4-MePy)$_4$(NCS)$_2$]-PX; (f) calculated and experimental PXRD patterns of the porous phase, [Ni(4-MePy)$_4$(NCS)$_2$]-**β′**.

P/P_0 (*i.e.*, *in vacuo*). The PXRD data demonstrated that immersing [Ni(4-MePy)$_4$(NCS)$_2$]-**α** in PX liquid afforded the same phase as PX vapor exposure (Fig. 2c). TGA data indicated that the PX molecule is released at 60 °C, followed by the degradation of [Ni(4-MePy)$_4$(NCS)$_2$]-PX (Fig. S2†). After the first adsorption–desorption cycle, both samples were subjected to a second PX sorption cycle (Fig. 2e) and both exhibited type I sorption isotherms as typically observed in rigid microporous materials,[76] with sharp uptake at the first data point (1% P/P_0). This sorption behavior can be repeated for at least three cycles (Fig. S5†), indicating the formation of a porous phase, [Ni(4-MePy)$_4$(NCS)$_2$]-**β′** (Fig. 2d), after the desorption process in the first cycle. This was subsequently corroborated by the matching calculated and experimental PXRD patterns (Fig. 2f).

With respect to the structural changes of [Ni(4-MePy)$_4$(NCS)$_2$] during phase transformations, crystallographic analysis of the reported crystal structures revealed that **α** crystallized in the monoclinic $P2_1/c$ space group, while **β** and **β′** crystallized in the tetragonal $I4_1/a$ space group (Table S2†). The [NiN$_6$] octahedral geometry remains almost consistent ($d_{Ni\cdots NCS}$ = 2.055–2.078 Å and $d_{Ni\cdots Npy}$ = 2.127–2.142 Å) among the **α**, **β** and **β′** phases (Fig. S6–S8†). However, the orientation of NCS$^-$ towards Ni(II) (*i.e.*, $\angle_{Ni-N-CS}$ angles) and the rotation of the pyridyl rings (*i.e.*, dihedral angles with the equatorial plane of [Ni(N$_{py}$)$_4$]) vary to some extent (Fig. S9–S11†). For the **α**, **β** and **β′** phases, the $\angle_{Ni-N-CS}$ angles are 156.87/163.69°, 162.99° and 152.81° and the dihedral angles are 50.01/56.40/56.51/59.93°, 46.72/55.19°, and 50.02/55.87°, respectively. Consequently, the differences in $\angle_{Ni-N-CS}$ and dihedral angles among these three phases are up to 10.88° and 13.21°, respectively. These variations highlight the structural flexibility of [Ni(4-MePy)$_4$(NCS)$_2$], despite its seemingly simple components.

During PX adsorption, the crystal volume of [Ni(4-MePy)$_4$(NCS)$_2$]-**α** underwent a significant increase of 18.1% to accommodate PX molecules (Fig. 3a and b). This expansion is made possible by rearranging the relative positions and orientations of individual [Ni(4-MePy)$_4$(NCS)$_2$] molecules (Fig. S12–S14†). For instance, the Ni⋯Ni distance between two adjacent [Ni(4-MePy)$_4$(NCS)$_2$] molecules increased from 8.41 to 12.58 Å (Fig. 3d and e). PX molecules were found to occupy channel cavities in the host structure (Fig. S15a†) and no significant guest–guest and/or host–guest interactions (*e.g.*, hydrogen bonding, π–π stacking), except for weak van der Waals forces, were observed. Therefore, it is unsurprising that PX was easily removed by applying a vacuum at room temperature as indicated by the PX vapor sorption tests. After PX desorption, the **β′** phase was found to contain 14.2% cage-type voids (Fig. S15b†) and experienced a slight contraction ($d_{Ni\cdots Ni}$ = 11.95 Å) in its structure (Fig. 3c and f) compared to the PX-loaded **β** phase.

[Ni(4-MePy)$_4$(NCS)$_2$]-**β′** was subjected to the sorption of a variety of guest species such as CH$_4$, C$_2$H$_6$, CH$_3$Cl and MeOH, with uptakes of around 1.5–1.9 mol mol^{-1}.[51] To further investigate the gas sorption behaviour of [Ni(4-MePy)$_4$(NCS)$_2$]-**β′**, we collected sorption isotherms for three industrially relevant C3 gases, C$_3$H$_4$ (propyne), C$_3$H$_6$ (propene), and C$_3$H$_8$ (propane), at both 273 and 298 K (Fig. 4a and b). This study revealed that [Ni(4-MePy)$_4$(NCS)$_2$]-**β′** exhibited similar affinities to all three C3 gases at low pressure (<5 kPa), suggesting low sorption selectivity. However, their sorption uptakes varied somewhat, with values of 64.7/43.7, 37.2/26.0 and 24.6/

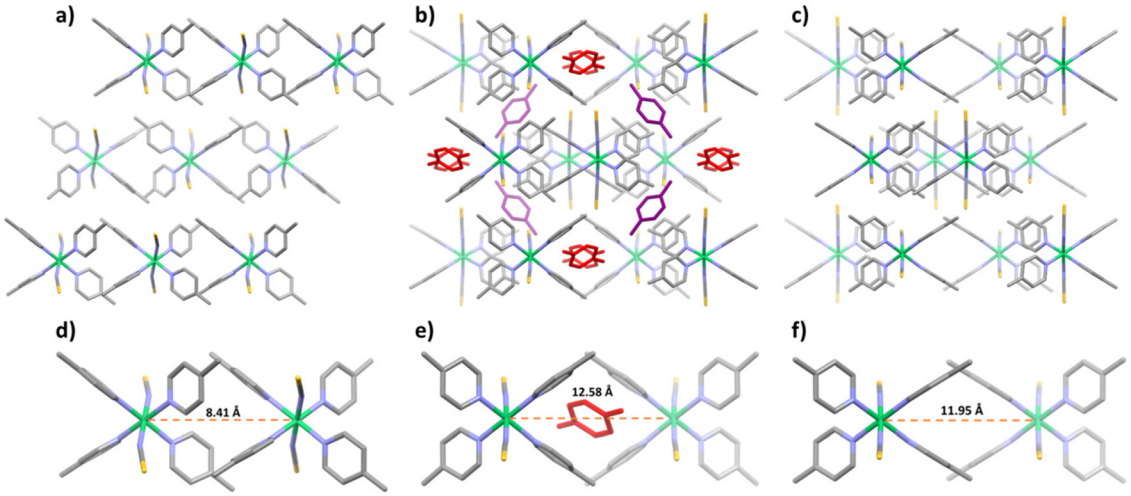

Fig. 3 The crystal packing (viewed along the *b* axis) for the **α** (a and d), **β** (b and e) and **β′** (c and f) phases of [Ni(4-MePy)$_4$(NCS)$_2$]. PX molecules are colored in red and purple.

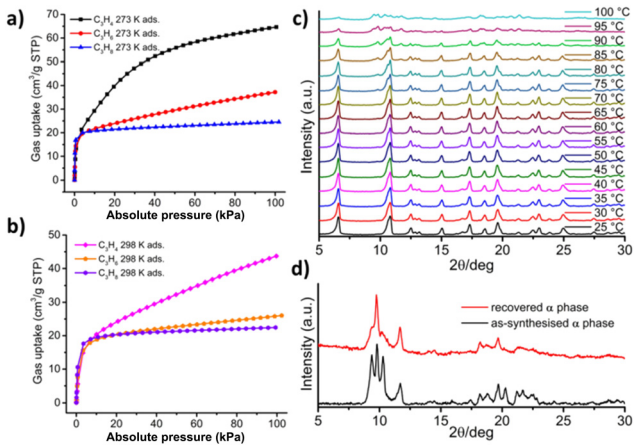

Fig. 4 C_3H_4, C_3H_6 and C_3H_8 adsorption isotherms at (a) 273 and (b) 298 K. For clarity, the desorption branches are omitted as they neatly overlay the corresponding adsorption branches. (c) VT-PXRD patterns of [Ni(4-MePy)$_4$(NCS)$_2$]-**β′**; and (d) PXRD patterns of the as-synthesised and recovered forms of [Ni(4-MePy)$_4$(NCS)$_2$]-**α**.

22.5 cm^3 g^{-1} for C_3H_4, C_3H_6 and C_3H_8, respectively, at 273/298 K, corresponding to 1.58/1.07, 0.91/0.63 and 0.60/0.55 mol mol^{-1}. These results indicate that temperature has varying influences on the sorption uptake of C_3H_4, C_3H_6 and C_3H_8. Furthermore, when combining these findings with previously reported CH_4 and C_2H_6 sorption data, which revealed uptakes of up to 1.9 and 1.8 mol mol^{-1} respectively,[51] it is evident that the shape/size of guest molecules impacts the sorption uptake of **β′**.

In terms of gas sorption on the **α** phase, to the best of our knowledge, only 195 K CO_2 sorption has been previously reported,[52] without any observed phase transformation. Given the potential for C_3H_4 to exhibit relatively strong host–guest interactions and induce structural transformations,[36] we collected C_3H_4 sorption data on [Ni(4-MePy)$_4$(NCS)$_2$]-**α** at 273 K up to 1 bar (Fig. S16†). No phase switching was observed.

We wondered if [Ni(4-MePy)$_4$(NCS)$_2$]-**β′** reverts to [Ni(4-MePy)$_4$(NCS)$_2$]-**α** by applying a second stimulus such as heat. Variable-temperature PXRD (VT-PXRD) experiments were therefore conducted under a laboratory atmosphere (Fig. 4c), which revealed that **β′** did not revert to **α** before degradation at 100 °C. Similar challenges were encountered in other shape-memory FMOMs.[44–46] To address this issue, we adopted a previously reported method by heating [Ni(4-MePy)$_4$(NCS)$_2$]-**β′** in a sealed pan at 80 °C,[65] which triggered its transformation to [Ni(4-MePy)$_4$(NCS)$_2$]-**α** (Fig. 4d). Nevertheless, we note that the recovered **α** form degraded at 16% P/P_0 when we attempted to conduct recyclability testing (Fig. S17†).

It is of importance to understand the existence of the metastable **β′** phase in the context of the shape-memory mechanism. From a thermodynamic standpoint, the dense **α** phase appears to be more stable, and previous studies have determined the enthalpy change between the **α** and **β′** phases to be around 3.3–5.0 kJ mol^{-1}.[65,77] This agrees with our DFT calculations, which afforded an enthalpy change of 5.0 kJ mol^{-1} (Fig. S18†). However, the energy barrier associated with the transition could be significantly higher, given that the structural transformations between the **α** and **β′** polymorphs require large translational and rotational movements due to their fundamentally different packing modes. Monitoring these transformations using *in situ* techniques could provide further insights.[29] This characteristic might contribute to the kinetically stable nature of **β′** at room temperature, as was demonstrated for [Cu$_2$(bdc)$_2$(bpy)]$_n$.[41] Moreover, **β′** and **β** only exhibit minor differences in the molecular structure of [Ni(4-MePy)$_4$(NCS)$_2$] (Fig. S11†) and practically no difference in their crystal packing (Fig. S13 and S14†). This structural similarity could help to explain why the guest-loaded **β** phases transform into the metastable **β′** phase during guest desorption.

Conclusions

In summary, we report herein the phase switching behaviour and shape-memory effect of $[Ni(4\text{-}MePy)_4(NCS)_2]$ induced by PX vapor sorption. C_3H_x gas sorption studies on the **β′** phase revealed guest size/shape-dependent sorption behaviour, with sorption uptakes being influenced differently by the temperature. Perhaps because multi-cycle successive sorption tests were rarely conducted in previous studies and the differences between the first and following sorption cycles remain virtually undiscovered, such shape-memory behavior has not been seen in other Werner complexes such as the 4-ethylpyridine and 4-vinylpyridine based analogues.[51,78] However, overall it is quite possible that shape-memory effects might be much more common than previously thought in molecular materials, considering the extensive exploration of supramolecular complexes/polymorphs in relation to host–guest interactions.[79–82] For example, a well-known organic macrocycle, *p-tert*-butylcalix-[4]arene, was recently reinvestigated with respect to the pore-shape fixing effects using the stimuli of CO_2 pressure and temperature.[83]

With respect to other potential guest stimuli, we found that $[Ni(4\text{-}MePy)_4(NCS)_2]$-**α** is fairly soluble or degradable in *o*/*m*-xylene isomers, which precluded study of their vapor sorption properties (Fig. S19†). Nevertheless, toluene was found to initiate the phase switching and shape-memory effect of $[Ni(4\text{-}MePy)_4(NCS)_2]$ (Fig. S20†). Various other guest molecules listed in Table S1† have been reported to form **β** phases, making them promising candidates as trigger molecules. Furthermore, investigation of the Co analogue ($[Co(4\text{-}MePy)_4(NCS)_2]$) could also offer insights; however, it is thermally stable only up to 70 °C (Fig. S21†) and does not survive the vacuum ($<1 \times 10^{-4}$ torr) in our vapour sorption system (Fig. S22†). This issue could be addressed through ambient pressure vapour sorption, but it would be more desirable to investigate Werner complexes with better thermal stability. Studies to explore sorption in a much broader range of Werner complexes are therefore in progress.

Experimental section

Sample synthesis

$[Ni(4\text{-}MePy)_4(NCS)_2]$-**α** was prepared by the water slurry method. $Ni(SCN)_2$ (2.5 mmol, 437 mg) and 4-methylpyridine (10 mmol, 931 mg) were added to 20 mL of water in a 30 mL vial. The slurry was stirred continuously for 3 h at room temperature and the solid was then filtered, washed with water and air-dried (yield ~95%). Part of the powder sample was recrystallized in hot ethanol to obtain large single crystals. The Co analogue was prepared by the same method, except that $Co(SCN)_2$ was used to replace $Ni(SCN)_2$.

Vapor sorption experiments

Xylene and water vapor sorption measurements were conducted using Surface Measurement Systems (SMS) DVS Vacuum or Intrinsic equipment at 298 K. Samples were degassed *in situ* and stepwise increases in relative pressure from 0 to 95% were controlled by equilibrated weight changes of the sample ($dM/dT = 0.01\%\ min^{-1}$). Approximately 10 mg of sample was used for each experiment. The mass change of the sample was recorded by a high-resolution microbalance with a precision of 0.1 μg.

Gas sorption experiments

C_3H_4, C_3H_6, and C_3H_8 gas sorption experiments were conducted on a Micromeritics 3flex instrument at 273 and 298 K. Around 80 mg of $[Ni(4\text{-}MePy)_4(NCS)_2]$-**β′** was used after degassing for 1 h. The temperature was maintained by a LAUDA Chiller.

Thermogravimetric analysis (TGA)

TGA was conducted under an N_2 atmosphere with a TA Instruments Q50 thermal analyzer between room temperature and 300 °C at a constant heating rate of 10 °C min^{-1}.

Powder X-ray diffraction (PXRD)

Powder X-ray diffraction experiments were conducted on a Panalytical Empyrean diffractometer (40 kV, 40 mA, Cu $K\alpha_{1,2}$, λ = 1.5418 Å) at room temperature with a range of $5° < 2\theta < 40°$.

Variable temperature powder X-ray diffraction (VT-PXRD)

VT-PXRD patterns were collected on Panalytical X'Pert diffractometer (40 kV, 40 mA, Cu $K\alpha_{1,2}$, λ = 1.5418 Å) at 5 °C intervals from 25 to 100 °C by heating at a rate of 5 °C min^{-1} under an air atmosphere. Diffraction patterns were collected in the 2θ range of 5–30°.

Scanning electron microscopy (SEM)

SEM analysis was performed using an SU 70 Hitachi instrument. The samples were sputter-coated with gold (20 mA, 90 s) prior to imaging.

Density functional theory (DFT) calculations

DFT calculations were performed using the SCAN + rVV10 method as implemented in the Vienna *ab initio* Simulation Package (VASP) software. This van der Waals density functional incorporated the rVV10 non-local correlation functional with the Strongly Constrained Appropriately Normed (SCAN) *meta*-GGA semi-local exchange–correlation functional, accounting for both short- and long-range interactions between the atoms of $[Ni(4\text{-}MePy)_4(NCS)_2]$ complexes in the closed **α** and open-empty **β′** phases. The projector augmented wave (PAW) method was used to describe electron–ion interactions, with plane-wave cutoffs of 500 eV. Atomic coordinates were relaxed in spin-unrestricted calculations until the calculated Hellmann–Feynman forces were under 0.001 eV $Å^{-1}$ and the energy tolerance reached 10^{-4} eV. For the Brillouin zone sampling, Γ-centered Monkhorst–Pack (MP) *k*-point meshes were used with densities around 20 *k*-points per Å.

Author contributions

Shi-Qiang Wang: methodology, investigation, formal analysis, and writing – original draft; Shaza Darwish: methodology, investigation, and writing – review & editing; Catiúcia R. M. O. Matos: investigation and writing – review & editing; Wong Zicong Marvin: investigation and writing – review & editing; Anjaiah Nalaparaju: investigation and writing – review & editing; Yifei Luo: investigation and writing – review & editing; Jun Zhu: investigation and writing – review & editing; Xiaofei Zhang: investigation and writing – review & editing; Zhengtao Xu: supervision, funding acquisition, and writing – review & editing; and Michael J. Zaworotko: supervision, funding acquisition, formal analysis, and writing – review & editing.

Conflicts of interest

There are no conflicts to declare.

Acknowledgements

M. J. Z. gratefully acknowledges the support of Science Foundation Ireland (16/IA/4624) and the Irish Research Council (IRCLA/2019/167). Z. X. acknowledges a startup fund from the Agency for Science, Technology and Research (SC25/22-119116). S.-Q. W. and Y. L. acknowledge the support from the Agency for Science, Technology and Research under the Manufacturing, Trade and Connectivity (MTC) Programmatic funding scheme (M23L8b0049).

References

1 S. Horike, S. Shimomura and S. Kitagawa, Soft porous crystals, *Nat. Chem.*, 2009, **1**, 695–704.
2 S. Krause, N. Hosono and S. Kitagawa, Chemistry of soft porous crystals: Structural dynamics and gas adsorption properties, *Angew. Chem., Int. Ed.*, 2020, **59**, 15325–15341.
3 S. Kitagawa, R. Kitaura and S. i. Noro, Functional porous coordination polymers, *Angew. Chem., Int. Ed.*, 2004, **43**, 2334–2375.
4 K. Uemura, R. Matsuda and S. Kitagawa, Flexible microporous coordination polymers, *J. Solid State Chem.*, 2005, **178**, 2420–2429.
5 A. J. Fletcher, K. M. Thomas and M. J. Rosseinsky, Flexibility in metal–organic framework materials: Impact on sorption properties, *J. Solid State Chem.*, 2005, **178**, 2491–2510.
6 S. Kitagawa and K. Uemura, Dynamic porous properties of coordination polymers inspired by hydrogen bonds, *Chem. Soc. Rev.*, 2005, **34**, 109–119.
7 G. Férey and C. Serre, Large breathing effects in three-dimensional porous hybrid matter: Facts, analyses, rules and consequences, *Chem. Soc. Rev.*, 2009, **38**, 1380–1399.
8 A. Schneemann, V. Bon, I. Schwedler, I. Senkovska, S. Kaskel and R. A. Fischer, Flexible metal–organic frameworks, *Chem. Soc. Rev.*, 2014, **43**, 6062–6096.
9 Z. Chang, D.-H. Yang, J. Xu, T.-L. Hu and X.-H. Bu, Flexible metal–organic frameworks: Recent advances and potential applications, *Adv. Mater.*, 2015, **27**, 5432–5441.
10 N. Behera, J. Duan, W. Jin and S. Kitagawa, The chemistry and applications of flexible porous coordination polymers, *EnergyChem*, 2021, **3**, 100067.
11 J. Dong, V. Wee and D. Zhao, Stimuli-responsive metal–organic frameworks enabled by intrinsic molecular motion, *Nat. Mater.*, 2022, **21**, 1334–1340.
12 J. A. Mason, J. Oktawiec, M. K. Taylor, M. R. Hudson, J. Rodriguez, J. E. Bachman, M. I. Gonzalez, A. Cervellino, A. Guagliardi, C. M. Brown, P. L. Llewellyn, N. Masciocchi and J. R. Long, Methane storage in flexible metal–organic frameworks with intrinsic thermal management, *Nature*, 2015, **527**, 357–361.
13 Q. Y. Yang, P. Lama, S. Sen, M. Lusi, K. J. Chen, W. Y. Gao, M. Shivanna, T. Pham, N. Hosono, S. Kusaka, J. J. t. Perry, S. Ma, B. Space, L. J. Barbour, S. Kitagawa and M. J. Zaworotko, Reversible switching between highly porous and nonporous phases of an interpenetrated diamondoid coordination network that exhibits gate-opening at methane storage pressures, *Angew Chem., Int. Ed.*, 2018, **57**, 5684–5689.
14 S.-Q. Wang, X.-Q. Meng, M. Vandichel, S. Darwish, Z. Chang, X.-H. Bu and M. J. Zaworotko, High working capacity acetylene storage at ambient temperature enabled by a switching adsorbent layered material, *ACS Appl. Mater. Interfaces*, 2021, **13**, 23877–23883.
15 M. Bonneau, C. Lavenn, J.-J. Zheng, A. Legrand, T. Ogawa, K. Sugimoto, F.-X. Coudert, R. Reau, S. Sakaki, K.-i. Otake and S. Kitagawa, Tunable acetylene sorption by flexible catenated metal–organic frameworks, *Nat. Chem.*, 2022, **14**, 816–822.
16 S.-Q. Wang, S. Darwish, X.-Q. Meng, Z. Chang, X.-H. Bu and M. J. Zaworotko, Acetylene storage performance of $[Ni(4,4'\text{-bipyridine})_2(NCS)_2]_n$, a switching square lattice coordination network, *Chem. Commun.*, 2022, **58**, 1534–1537.
17 Q. Dong, X. Zhang, S. Liu, R. B. Lin, Y. Guo, Y. Ma, A. Yonezu, R. Krishna, G. Liu, J. Duan, R. Matsuda, W. Jin and B. Chen, Tuning gate-opening of a flexible metal–organic framework for ternary gas sieving separation, *Angew Chem., Int. Ed.*, 2020, **59**, 22756–22762.
18 S.-Q. Wang, S. Mukherjee, E. Patyk-Kaźmierczak, S. Darwish, A. Bajpai, Q.-Y. Yang and M. J. Zaworotko, Highly selective, high-capacity separation of *o*-xylene from C8 aromatics by a switching adsorbent layered material, *Angew Chem. Int. Ed.*, 2019, **58**, 6630–6634.
19 H. Zeng, M. Xie, T. Wang, R.-J. Wei, X.-J. Xie, Y. Zhao, W. Lu and D. Li, Orthogonal-array dynamic molecular sieving of propylene/propane mixtures, *Nature*, 2021, **595**, 542–548.
20 Z. Wang, N. Sikdar, S.-Q. Wang, X. Li, M. Yu, X.-H. Bu, Z. Chang, X. Zou, Y. Chen, P. Cheng, K. Yu, M. J. Zaworotko

and Z. Zhang, Soft porous crystal based upon organic cages that exhibit guest-induced breathing and selective gas separation, *J. Am. Chem. Soc.*, 2019, **141**, 9408–9414.

21 X. Wang, R. Krishna, L. Li, B. Wang, T. He, Y.-Z. Zhang, J.-R. Li and J. Li, Guest-dependent pressure induced gate-opening effect enables effective separation of propene and propane in a flexible MOF, *Chem. Eng. J.*, 2018, **346**, 489–496.

22 L. Li, S. Zhao, H. Huang, M. Dong, J. Liang, H. Li, J. Hao, E. Zhao and X. Gu, Advanced soft porous organic crystal with multiple gas-induced single-crystal-to-single-crystal transformations for highly selective separation of propylene and propane, *Adv. Sci.*, 2024, **11**, 2303057.

23 C. R. Murdock, B. C. Hughes, Z. Lu and D. M. Jenkins, Approaches for synthesizing breathing MOFs by exploiting dimensional rigidity, *Coord. Chem. Rev.*, 2014, **258**, 119–136.

24 J.-P. Zhang, H.-L. Zhou, D.-D. Zhou, P.-Q. Liao and X.-M. Chen, Controlling flexibility of metal–organic frameworks, *Natl. Sci. Rev.*, 2018, **5**, 907–919.

25 J. H. Lee, S. Jeoung, Y. G. Chung and H. R. Moon, Elucidation of flexible metal-organic frameworks: Research progresses and recent developments, *Coord. Chem. Rev.*, 2019, **389**, 161–188.

26 I. Senkovska, V. Bon, L. Abylgazina, M. Mendt, J. Berger, G. Kieslich, P. Petkov, J. Luiz Fiorio, J.-O. Joswig, T. Heine, L. Schaper, C. Bachetzky, R. Schmid, R. A. Fischer, A. Pöppl, E. Brunner and S. Kaskel, Understanding MOF flexibility: An analysis focused on pillared layer MOFs as a model system, *Angew. Chem., Int. Ed.*, 2023, **62**, e202218076.

27 S. K. Elsaidi, M. H. Mohamed, D. Banerjee and P. K. Thallapally, Flexibility in metal–organic frameworks: A fundamental understanding, *Coord. Chem. Rev.*, 2018, **358**, 125–152.

28 Y. Li, Y. Wang, W. Fan and D. Sun, Flexible metal–organic frameworks for gas storage and separation, *Dalton Trans.*, 2022, **51**, 4608–4618.

29 V. Bon, E. Brunner, A. Pöppl and S. Kaskel, Unraveling structure and dynamics in porous frameworks via advanced in situ characterization techniques, *Adv. Funct. Mater.*, 2020, **30**, 1907847.

30 S.-Q. Wang, S. Mukherjee and M. J. Zaworotko, Spiers Memorial Lecture: Coordination networks that switch between nonporous and porous structures: An emerging class of soft porous crystals, *Faraday Discuss.*, 2021, **231**, 9–50.

31 L. Vanduyfhuys, S. Rogge, J. Wieme, S. Vandenbrande, G. Maurin, M. Waroquier and V. Van Speybroeck, Thermodynamic insight into stimuli-responsive behaviour of soft porous crystals, *Nat. Commun.*, 2018, **9**, 1–9.

32 Y. Huang, J. Wan, T. Pan, K. Ge, Y. Guo, J. Duan, J. Bai, W. Jin and S. Kitagawa, Delicate softness in a temperature-responsive porous crystal for accelerated sieving of propylene/propane, *J. Am. Chem. Soc.*, 2023, **145**, 24425–24432.

33 K. Koupepidou, V. I. Nikolayenko, D. Sensharma, A. A. Bezrukov, M. Shivanna, D. C. Castell, S.-Q. Wang, N. Kumar, K.-i. Otake, S. Kitagawa and M. J. Zaworotko, Control over phase transformations in a family of flexible double diamondoid coordination networks through linker ligand substitution, *Chem. Mater.*, 2023, **35**, 3660–3670.

34 N. Nijem, H. Wu, P. Canepa, A. Marti, K. J. Balkus, T. Thonhauser, J. Li and Y. J. Chabal, Tuning the gate opening pressure of metal–organic frameworks (MOFs) for the selective separation of hydrocarbons, *J. Am. Chem. Soc.*, 2012, **134**, 15201–15204.

35 S.-Q. Wang, S. Darwish, D. Sensharma and M. J. Zaworotko, Tuning the switching pressure in square lattice coordination networks by metal cation substitution, *Mater. Adv.*, 2022, **3**, 1240–1247.

36 S.-Q. Wang, S. Darwish and M. J. Zaworotko, Adsorbate-dependent phase switching in the square lattice topology coordination network $[Ni(4,4'\text{-bipyridine})_2(NCS)_2]_n$, *Chem. Commun.*, 2023, **59**, 559–562.

37 K. Otsuka and C. M. Wayman, *Shape memory materials*, Cambridge University Press, 1999.

38 L. Sun, W. M. Huang, Z. Ding, Y. Zhao, C. C. Wang, H. Purnawali and C. Tang, Stimulus-responsive shape memory materials: A review, *Mater. Des.*, 2012, **33**, 577–640.

39 J. Mohd Jani, M. Leary, A. Subic and M. A. Gibson, A review of shape memory alloy research, applications and opportunities, *Mater. Des.*, 2014, **56**, 1078–1113.

40 M. Behl, M. Y. Razzaq and A. Lendlein, Multifunctional shape-memory polymers, *Adv. Mater.*, 2010, **22**, 3388–3410.

41 Y. Sakata, S. Furukawa, M. Kondo, K. Hirai, N. Horike, Y. Takashima, H. Uehara, N. Louvain, M. Meilikhov and T. Tsuruoka, Shape-memory nanopores induced in coordination frameworks by crystal downsizing, *Science*, 2013, **339**, 193–196.

42 M. Shivanna, Q.-Y. Yang, A. Bajpai, S. Sen, N. Hosono, S. Kusaka, T. Pham, K. A. Forrest, B. Space, S. Kitagawa and M. J. Zaworotko, Readily accessible shape-memory effect in a porous interpenetrated coordination network, *Sci. Adv.*, 2018, **4**, eaaq1636.

43 M. Shivanna, Q.-Y. Yang, A. Bajpai, E. Patyk-Kazmierczak and M. J. Zaworotko, A dynamic and multi-responsive porous flexible metal–organic material, *Nat. Commun.*, 2018, **9**, 3080.

44 H. Yang, T. X. Trieu, X. Zhao, Y. Wang, Y. Wang, P. Feng and X. Bu, Lock-and-key and shape-memory effects in an unconventional synthetic path to magnesium metal–organic frameworks, *Angew Chem., Int. Ed.*, 2019, **58**, 11757–11762.

45 Y. Chen, K. B. Idrees, F. A. Son, X. Wang, Z. Chen, Q. Xia, Z. Li, X. Zhang and O. K. Farha, Tuning the structural flexibility for multi-responsive gas sorption in isonicotinate-based metal–organic frameworks, *ACS Appl. Mater. Interfaces*, 2021, **13**, 16820–16827.

46 K. Roztocki, W. Gromelska, F. Formalik, A. Giordana, L. Andreo, G. Mahmoudi, V. Bon, S. Kaskel, L. J. Barbour, A. Janiak and E. Priola, Shape-memory effect triggered by

π–π interactions in a flexible terpyridine metal–organic framework, *ACS Mater. Lett.*, 2023, **5**, 1256–1260.

47 B.-Q. Song, M. Shivanna, M.-Y. Gao, S.-Q. Wang, C.-H. Deng, Q.-Y. Yang, S. J. Nikkhah, M. Vandichel, S. Kitagawa and M. J. Zaworotko, Shape-memory effect enabled by ligand substitution and CO_2 affinity in a flexible SIFSIX coordination network, *Angew Chem., Int. Ed.*, 2023, **62**, e202309985.

48 Y. Shigeta, A. Kobayashi, T. Ohba, M. Yoshida, T. Matsumoto, H.-C. Chang and M. Kato, Shape-memory platinum(II) complexes: Intelligent vapor-history sensor with ON–OFF switching function, *Chem. – Eur. J.*, 2016, **22**, 2682–2690.

49 A. M. Kałuża, S. Mukherjee, S.-Q. Wang, D. J. O'Hearn and M. J. Zaworotko, [Cu(4-phenylpyridine)$_4$(trifluoromethanesulfonate)$_2$], a Werner complex that exhibits high selectivity for *o*-xylene, *Chem. Commun.*, 2020, **56**, 1940–1943.

50 C. R. M. O. Matos, R. Sanii, S.-Q. Wang, C. M. Ronconi and M. J. Zaworotko, Reversible single-crystal to single-crystal phase transformation between a new Werner clathrate and its apohost, *Dalton Trans.*, 2021, **50**, 12923–12930.

51 S. A. Allison and R. M. Barrer, Sorption in the β-phases of transition metal(II) tetra-(4-methylpyridine) thiocyanates and related compounds, *J. Chem. Soc. A*, 1969, 1717–1723.

52 S.-i. Noro, T. Ohba, K. Fukuhara, Y. Takahashi, T. Akutagawa and T. Nakamura, Diverse structures and adsorption properties of quasi-Werner-type copper(II) complexes with flexible and polar axial bonds, *Dalton Trans.*, 2011, **40**, 2268–2274.

53 M. Lusi and L. J. Barbour, Solid-vapor sorption of xylenes: prioritized selectivity as a means of separating all three isomers using a single substrate, *Angew. Chem., Int. Ed.*, 2012, **51**, 3928–3931.

54 S.-i. Noro, K. Fukuhara, K. Sugimoto, Y. Hijikata, K. Kubo and T. Nakamura, Anion-dependent host-guest properties of porous assemblies of coordination complexes (PACs), [Cu(A)$_2$(py)$_4$] (A = PF_6, BF_4, CF_3SO_3, and CH_3SO_3; py = pyridine), based on Werner-type copper(II) complexes in the solid state, *Dalton Trans.*, 2013, **42**, 11100–11110.

55 S.-i. Noro, Y. Song, Y. Tanimoto, Y. Hijikata, K. Kubo and T. Nakamura, Controlling the gate-sorption properties of solid solutions of Werner complexes by varying component ratios, *Dalton Trans.*, 2020, **49**, 9438–9443.

56 J. E. D. Davies, W. Kemula, H. M. Powell and N. O. Smith, Inclusion compounds—Past, present, and future, *J. Inclusion Phenom.*, 1983, **1**, 3–44.

57 J. Lipkowski, Inclusion compounds formed by Werner MX2A4 coordination complexes, in *Inclusion Compounds: Structural Aspects of Inclusion Compounds Formed by Inorganic and Organometallic Host Lattices*, ed. J. L. Atwood, J. E. D. Davies and D. D. MacNicol, Academic Press, London, 1984, Vol. 1, pp. 59–103.

58 A. V. Logan and D. W. Carle, The preparation of nickel(II) thiocyanate complex compounds with picolines and the determination of their heats of formation, *J. Am. Chem. Soc.*, 1952, **74**, 5224–5225.

59 I. S. Kerr and D. J. Williams, α-Tetrakis(4-methylpyridine)-diisothiocyanatonickel(II), *Acta Crystallogr., Sect. B: Struct. Crystallogr. Cryst. Chem.*, 1977, **33**, 3589–3592.

60 W. D. Schaeffer, W. S. Dorsey, D. A. Skinner and C. G. Christian, Separation of xylenes, cymenes, methylnaphthalenes and other isomers by clathration with inorganic complexes, *J. Am. Chem. Soc.*, 1957, **79**, 5870–5876.

61 F. V. Williams, Clathrate compounds of Werner complexes with p-disubstituted benzene derivatives, *J. Am. Chem. Soc.*, 1957, **79**, 5876–5877.

62 D. Belitskus, G. A. Jeffrey, R. K. McMullan and N. C. Stephenson, Single crystal studies on some clathrates of tetra-(4-methylpyridine)-nickel(II) and cobalt dithiocyanates, *Inorg. Chem.*, 1963, **2**, 873–875.

63 J. Lipkowski, K. Suwińska, G. D. Andreetti and K. Stadnicka, Clathrate inclusion compounds of bis (isothiocyanato) tetrakis (4-methylpyridine) nickel II: II. Arrangement of guest molecules in the β-Ni(NCS)$_2$(4-methylpyrldine)$_4$ porous crystals, *J. Mol. Struct.*, 1981, **75**, 101–112.

64 A. Y. Manakov, J. Lipkowski, K. Suwinska and M. Kitamura, New crystal structures of β-[Ni(NCS)$_2$(4-methylpyridine)$_4$] clathrates with furan, tetrahydrofuran, methylene chloride, benzene + ethanol and methylcellosolve as guest molecules, *J. Inclusion Phenom. Mol. Recognit. Chem.*, 1996, **26**, 1–20.

65 D. V. Soldatov, G. D. Enright and J. A. Ripmeester, Polymorphism and Pseudopolymorphism of the [Ni(4-methylpyridine)$_4$(NCS)$_2$] Werner complex, the compound that led to the concept of "organic zeolites", *Cryst. Growth Des.*, 2004, **4**, 1185–1194.

66 G. D. Andreetti, G. Bocelli and P. Sgarabotto, Bis (Isothiocyanato) tetrakis(4-methylpyridine) nickel(II) $C_{26}H_{28}N_6NiS_2$, *Cryst. Struct. Commun.*, 1972, **1**, 51–54.

67 M. I. Hart and N. O. Smith, Thermodynamics and structure of the p-xylene and p-dichlorobenzene clathrates of tetra-(4-methylpyridine)-nickel(II) thiocyanate, *J. Am. Chem. Soc.*, 1962, **84**, 1816–1819.

68 G. D. Jacobs and M. T. Lok, Properties of some Werner-complex clathrates utilizing tetrakis (4-methylpyridine) metal(II) thiocyanate (metal = nickel, cobalt, iron, manganese), *Inorg. Chem.*, 1971, **10**, 1823–1825.

69 M. Rahmani, C. R. M. O. Matos, S.-Q. Wang, A. A. Bezrukov, A. C. Eaby, D. Sensharma, Y. Hjiej-Andaloussi, M. Vandichel and M. J. Zaworotko, Highly selective p-xylene separation from mixtures of C8 aromatics by a nonporous molecular apohost, *J. Am. Chem. Soc.*, 2023, **145**, 27316–27324.

70 A.-X. Zhu, Q.-Y. Yang, A. Kumar, C. Crowley, S. Mukherjee, K.-J. Chen, S.-Q. Wang, D. O'Nolan, M. Shivanna and M. J. Zaworotko, Coordination network that reversibly switches between two nonporous polymorphs and a high surface area porous phase, *J. Am. Chem. Soc.*, 2018, **140**, 15572–15576.

71 H. Miura, V. Bon, I. Senkovska, S. Ehrling, S. Watanabe, M. Ohba and S. Kaskel, Tuning the gate-opening pressure

and particle size distribution of the switchable metal–organic framework DUT-8(Ni) by controlled nucleation in a micromixer, *Dalton Trans.*, 2017, **46**, 14002–14011.

72 L. Abylgazina, I. Senkovska, S. Ehrling, V. Bon, P. St. Petkov, J. D. Evans, S. Krylova, A. Krylov and S. Kaskel, Tailoring adsorption induced switchability of a pillared layer MOF by crystal size engineering, *CrystEngComm*, 2021, **23**, 538–549.

73 X. Yang, H.-L. Zhou, C.-T. He, Z.-W. Mo, J.-W. Ye, X.-M. Chen and J.-P. Zhang, Flexibility of metal–organic framework tunable by crystal size at the micrometer to sub-millimeter scale for efficient xylene isomer separation, *Research*, 2019, **2019**, 9463719.

74 S.-Q. Wang, S. Darwish and M. J. Zaworotko, The impact of solution vs. slurry vs. mechanochemical syntheses upon the sorption performance of a 2D switching coordination network, *Inorg. Chem. Front.*, 2023, **10**, 3821–3827.

75 M.-Y. Gao, A. A. Bezrukov, B.-Q. Song, M. He, S. J. Nikkhah, S.-Q. Wang, N. Kumar, S. Darwish, D. Sensharma, C. Deng, J. Li, L. Liu, R. Krishna, M. Vandichel, S. Yang and M. J. Zaworotko, Highly productive C_3H_4/C_3H_6 trace separation by a packing polymorph of a layered hybrid ultramicroporous material, *J. Am. Chem. Soc.*, 2023, **145**, 11837–11845.

76 M. Thommes, K. Kaneko, A. V. Neimark, J. P. Olivier, F. Rodriguez-Reinoso, J. Rouquerol and K. S. Sing, Physisorption of gases, with special reference to the evaluation of surface area and pore size distribution (IUPAC Technical Report), *Pure Appl. Chem.*, 2015, **87**, 1051–1069.

77 J. Liprowski, P. Starzewski and W. Zielenkiewicz, Thermochemical studies of the clathration of aromatic guest compounds by the host—$Ni(NCS)_2$(4-methylpyridine)$_4$ complex, *Thermochim. Acta*, 1981, **49**, 269–279.

78 E. Rodulfo de Gil and I. S. Kerr, A comparison of the porosities of the [beta]-phases of (4-methylpyridine)$_4Ni(NCS)_2$ and (4-vinylpyridine)$_4Co(NCS)_2$, *J. Appl. Crystallogr.*, 1977, **10**, 315–320.

79 B. Moulton and M. J. Zaworotko, From molecules to crystal engineering: supramolecular isomerism and polymorphism in network solids, *Chem. Rev.*, 2001, **101**, 1629–1658.

80 L. R. Nassimbeni, Physicochemical aspects of host–guest compounds, *Acc. Chem. Res.*, 2003, **36**, 631–637.

81 S. J. Dalgarno, P. K. Thallapally, L. J. Barbour and J. L. Atwood, Engineering void space in organic van der Waals crystals: Calixarenes lead the way, *Chem. Soc. Rev.*, 2007, **36**, 236–245.

82 K. Jie, Y. Zhou, E. Li and F. Huang, Nonporous adaptive crystals of pillararenes, *Acc. Chem. Res.*, 2018, **51**, 2064–2072.

83 A. C. Eaby, L. Loots, J. L. Basson, C. Esterhuysen and L. J. Barbour, Programmed pore-shape fixing in a soft porous molecular crystal—navigating the phase interconversion landscape, *Angew. Chem., Int. Ed.*, 2023, **62**, e202304152.

